Nonequilibrium molecular dynamics simulation of gas-mixtures transport in carbon-nanopore membranes

I. V. Kaganov and M. Sheintuch
Department of Chemical Engineering, Technion-IIT, Haifa 32000, Israel
(Received 23 February 2003; published 2 October 2003)

The numerical simulation of nonequilibrium cotransport of H_2 and alkane gas mixtures with very different molecular sizes through a porous carbon membrane structure was implemented. Simulated permeabilities and selectivities in binary diffusive systems (and in one ternary system), at pressure about tens of atmospheres and at operating condition of room temperature or higher, can be predicted from single-gas permeabilities. This suggests that the effect is geometrical and an approximate model of the transport is proposed. It can be used for an estimation of the separation factor of a membrane. Simulations are compared with experimental results of two- and three-component codiffusion and counterdiffusion in a carbon membrane. It is shown that diffusion in a porous molecular network and in a carbon nanotube are completely different. The uniqueness of this work lies in the comparison of simulated, approximate, and experimental results, which enables us to identify the important parameters.

DOI: 10.1103/PhysRevE.68.046701 PACS number(s): 02.70.Ns, 05.60.Cd, 47.55.Mh

I. INTRODUCTION

Transport of gas mixtures through porous membranes and especially through molecular sieves is a subject of great current interest [1]. Membranes are used in separation and in catalytic processes in which a mixture of compounds is involved. Such porous membranes contain a range of pore sizes. The most promising class of membranes for the purpose of gas separation is the one with nanopores in which a significant separation can be achieved.

This paper deals with one class of such porous materials—carbon molecular-sieve membranes. Carbon membranes are molecular sieves that incorporate pores of molecular dimensions so that steric and other effects, associated with the proximity of the pore wall, play an increasingly important role in transport processes. Adsorption tests showed that the pore structure is composed from relatively wide pores separated by few constrictions responsible for the molecular-sieving effect [2]. The importance of this class of membranes stems from the good ratio of price to quality which makes them potential candidates for a number of commercial applications [2–4]. Many factors, such as pore size distribution, the interconnection of the pores, the identity of species, and the operating temperature contribute to the overall transport properties. Gas separation is a nonequilibrium complex process, and a quantitative description of transport in such membranes, which can predict fluxes and selectivities, has not been developed yet. The molecular dynamics simulation seems currently to be the only valid tool for studying these processes.

This paper attempts to predict the transport selectivities (the ratio of permeabilities) of hydrogen and C_1H_4–C_4H_{10} alkanes achieved by a carbon membrane. The simulations use a porous membrane model and apply dual control volume nonequilibrium molecular dynamics methods for this purpose. The choice of these techniques is argued below. The experimental motivations for our study are measurements of permeabilities and selectivities in a molecular-sieve carbon membrane hollow-fiber module at the temperature range of 25 °C–400 °C; nitrogen is used as a sweeping gas in the study of mixtures. The separation experiment was conducted at steady state with nitrogen flowing on the tube side and a hydrogen/alkane mixture on the shell side. The fluxes of pure components are studied under a pressure gradient. The membrane selectivity, i.e., the ratio of hydrogen to hydrocarbon permeabilities, may reach 100–1000 in propane or in (normal- or iso-) butane mixtures with hydrogen, making the membrane an excellent candidate for a membrane dehydrogenation reactor. The permeabilities measured in pure-component studies differ from those in mixtures: Specifically, counterdiffusion of nitrogen and C_1H_4–C_4H_{10} alkanes significantly inhibits the fluxes of both, while hydrogen flux is only slightly diminished; the experimental results are presented elsewhere [5].

In choosing the molecular dynamics (MD) approach that will best describe the experimental system we can choose between a slit and a nanotube representation of a single pore and between equilibrium and nonequilibrium methods. A number of studies of transport processes in nanopore membranes may be found in literature. These are equilibrium simulations which do not resemble the experimental study described here and mostly impose specific conditions [6–10] (e.g., gases are differed only in their ''colors,'' periodic boundary conditions are imposed in flow direction, etc.) and a number of nonequilibrium simulations of the transport through a single pore. The differences between equilibrium (MD) and nonequilibrium MD (NEMD) approaches have been extensively debated, and some studies show that diffusivities predicted by these approaches can differ by one order or several orders of magnitude [19]. There is an agreement that diffusion under a concentration gradient is better described by NEMD. The diffusion through the slit pore [11] and the motion through a cylindrical pore [12,13] were studied; see also Ref. [14]. The actual carbon membrane, however, is a porous network and this fact must be accounted for if one hopes to reach some quantitative description of an experimental situation (Ref. [11] show that single-pore simu-

lation underestimates the separation factors by one order or even two orders of magnitude and discuss these issues; see also Refs. [15,16]).

If one decides to generate the molecular pore network (in simulation), then a specific method should be chosen. Sahimi and co-workers constructed a network of so called ''pillared clays'' [17], which is essentially a two-dimensional network and does not relate to our study. In another work they used the Voronoi tesselation to describe carbon membrane [15,18]: a number of uniformly distributed random points (Poisson points) were inserted into the graphite structure of membrane and the polyhedra near each of them were built. To obtain the desired distribution of pore sizes, which is claimed not to be Gaussian [11], a method of sorting these polyhedra according to their sizes was suggested. A number of such polyhedra was emptied after that to create pore space.

In this paper we construct a pore network with Poisson distribution of sizes: this results in a distribution similar to the actual (and biased to the smallest sizes of course) without resorting to any artificial procedure. This paper also differs from those cited above, in that it deals with various molecular sizes of gases including some that are larger than the average pore size. Since entering and leaving the pore space (adsorption and desorption) may be rate limiting, we use the dual control volume (DCV)-NEMD approach. The transport selectivity is determined then by pure geometric factors when the molecule-solid (attractive) interaction is negligible or by energetic consideration when the interaction is important.

The structure of this work is as follows. The solid model and molecular dynamics simulation code are described below, followed by the main results. A crude geometric model is discussed in Sec. IV. The separation experiment was conducted at steady state in a commercial module of a hollow-fiber carbon tube with N_2 flowing on the tube side and the hydrogen/alkane mixture on the shell side. The uniqueness of this work lies in the comparison of simulated, approximate, and experimental results, which enables us to identify the important parameters.

II. THE MODEL AND NUMERICAL SIMULATION

A molecular dynamics simulation was implemented here, using the grand-canonical molecular dynamics method [20] and a DCV technique [21,22], as will be described below.

The volume where simulation was implemented was designed as the parallelepiped with a rhombus having $L=aN$ side and $\pi/3$ angle as its basis. This shape was chosen to be consistent with the graphite structure of the porous media; here a is the distance between the nearest carbon atoms in graphite, and N is an integer that specifies the size of simulated volume. The height of the parallelepiped is divided into three parts: two control volumes and a porous membrane space between them. The heights of the control volumes are $L_1=cN_1$ and the height of the middle part is $L_1'=cN_1'$, where c is the double distance between graphite planes and N_1 and N_1' are integers which specify the size of the simulation cell. Let the main direction along the height of the parallelepiped be the z direction and let us impose periodic boundary conditions in the x, y directions. Each control volume is ''filled'' with an equilibrium mixture of gases; a concentration gradient between the volumes creates the driving force for diffusion.

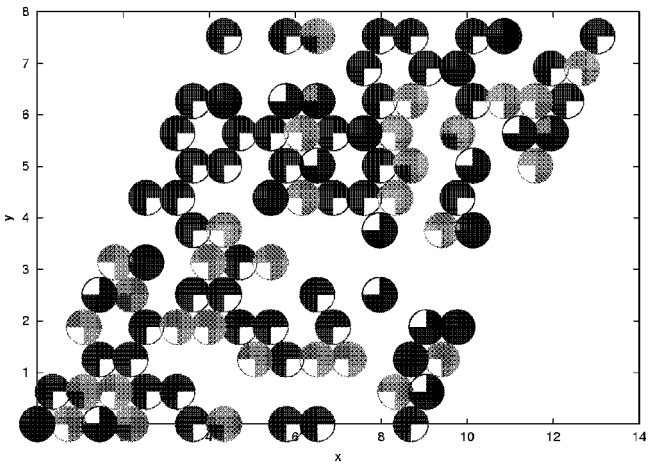

FIG. 1. Example of carbon membrane structure (three layers, z direction is perpendicular to the plane of paper) The gray circles present lower level, the light gray ones present middle level, and the black ones present upper level.

The membrane construction followed experimental observations [23]: A graphite ''block'' was generated between the control volumes. To create porosity, a number of carbon atoms in spheres, having a Poisson distribution of atoms inside and a uniform random distribution of center positions, were removed. Thus, the procedure consisted of the subsequent generations of spheres with center positions inside the membrane and random volumes and deletions of atoms inside them. The parameter of the Poisson distribution of absent atoms inside pores (average number of absent atoms) was kept constant. The sequence of Poisson distributed numbers with a given average was generated using a standard algorithm. A typical example of the resulting structure is displayed at Fig. 1; the smoothed distribution of the pore sizes (diameters) is shown at Fig. 2. The specific distribution of pore sizes is described by an average pore size d; the procedure is completed when the given porosity p has been reached (here $p=n_e/n_t$, n_e is the number of removed atoms, and n_t is the initial number of carbon atoms). Thus, a porous atomic network with a predetermined porosity and average pore size was created. This method is different from that described before [15] and is more natural. It should be a good approximation of a pore network in chemically activated carbon, which resembles the experimental studies [5]. Chemically activated carbons are produced by mixing an activation chemical with a carbonaceous material and carbonizing the resultant mixture. The result is a very porous carbon structure filled with an activation agent. The latter is removed from the carbon by washing. As a result of the relatively low process temperature, graphitic basal planes are not found in chemically activated carbons. The pore walls are thus not flat but ''rough.'' If one assumes that carbon atoms are removed independently, then the resulting distribution of pore volumes will be of the Poisson type.

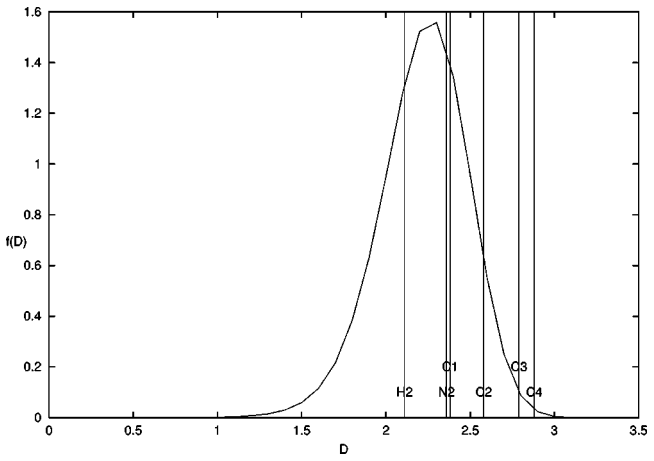

FIG. 2. Smoothed distribution f of the pore diameter D in dimensionless units; $\langle D\rangle = d = 2.25$. The distribution is normalized: $\int_0^\infty f(D)dD = 1$ The vertical lines show the lower cutoffs of pore size for passage of H_2, N_2, CH_4, C_2H_6, C_3H_8, and i-C_4H_{10} from left to right accordingly

The two control volumes were filled with a mixture of gaseous H_2 and an alkane gas having the same temperature in both control volumes but different chemical potentials.

The approximation of Lennard-Jones (LJ) potential of intermolecular interaction was employed here. This is justified since even the transport of such clear nonspherical molecules as CO_2 may be adequately described by LJ potential [11]. The interaction between molecules of different gases and carbon atoms of the solid membrane was described using the shifted LJ potential

$$U(r) = U_{LJ}(r) - U_{LJ}(r_c), \tag{1}$$

where $U_{LJ}(r) = 4\epsilon[(\sigma/r)^{12} - (\sigma/r)^6]$, r_c was chosen to be as large as $4\sigma_c$, where σ_c is the LJ parameter of carbon atom. Then the corrections due to the shift and cut (at $r > r_c$) should be negligible. The interaction between molecules (and atoms) of different species was described by the Lorentz-Berthelot rule $\epsilon_{ij} = \sqrt{\epsilon_i \epsilon_j}$ and $\sigma_{ij} = (\sigma_i + \sigma_j)/2$.

For the purpose of simulation the following scales were chosen: for the unit of energy ϵ_c we used the LJ parameter of carbon atom ($\epsilon_c/k = 28$ K) [11], the distance unit was $\sigma_c = 0.34$ nm [11], $\hbar$ was established to be 1 and so the mass unit became $\hbar^2/\epsilon_c\sigma_c^2 = 0.150$ a.m.u., the time unit was $\hbar/\epsilon_c$, and the temperature was measured in energy units (k is the Boltzmann constant here).

The parameters of the considered gases were taken from the literature [24]. They are given (in dimensionless units) in the Table I (m is the mass of molecules). In dimensionless units $a = 0.724$, $c = 1.97$.

TABLE I. LJ parameters of simulated gases.

	H_2	CH_4	C_2H_6	C_3H_8	i-C_4H_{10}	N_2
σ	0.88	1.12	1.30	1.49	1.57	1.10
ϵ	1.36	4.89	8.21	9.07	11.2	2.86
m	13.3	107	200	293	387	187

The simulation was conducted using the combined Monte Carlo and molecular dynamics technique: Monte Carlo insertions and deletions of particles were performed inside the control volumes until equilibrium μVT ensembles were created; after that one step of molecular dynamics was done using Beeman algorithm [25] and the cycle was repeated. Because of periodic boundary conditions in the x and y directions, the only way for a particle to leave the simulated volume was to cross the outer boundaries in z direction. Such particles were removed from consideration but were used to calculate the partial pressures of gases.

During Monte Carlo stage, the particles were inserted and deleted (different species of particles with equal chances) with the probabilities [25]

$$N_\alpha \to N_\alpha + 1 : \min\left(1, \frac{VZ_\alpha(T)}{N_\alpha + 1} e^{(U_{N_\alpha} - U_{N_\alpha + 1})/T}\right),$$

$$N_\alpha \to N_\alpha - 1 : \min\left(1, \frac{N_\alpha}{VZ_\alpha(T)} e^{(U_{N_\alpha} - U_{N_\alpha - 1})/T}\right) \tag{2}$$

(expressing the condition that a particle appears or disappears basically if, as a result, the total energy of the system declines). Here α denotes the kind of particles, N_α denotes the number of particles of the type α, V is the control volume, $Z_\alpha(T) = e^{\mu_\alpha/T}(m_\alpha T/2\pi\hbar^2)^{3/2}$, T is the temperature, μ_α is the chemical potential of the particles of sort α in the current control volume, m_α is the mass of the particles of sort α, and U_{N_α} is the total interaction energy of the system with N_α particles of sort α in the given control volume. The place where the new particle is attempted to be inserted inside the control volume or the ordinal number of particle inside the control volume which is attempted to be removed is chosen uniformly randomly. Each new particle obtained a velocity consistent with the Maxwell distribution at a given temperature T. An equilibrium was assumed to be established when the difference between the numbers of insertions and deletions during Monte Carlo process, of any species of particles in each control volume, was smaller than 5%.

After that the new positions and velocities were calculated using the Beeman algorithm and taking into account the periodic boundary conditions:

$$x^n_{\alpha ji} = x^c_{\alpha ji} + v^c_{\alpha ji}\Delta t + \frac{4f^c_{\alpha ji} - f^p_{\alpha ji}}{6m_\alpha}(\Delta t)^2,$$

$$v^n_{\alpha ji} = v^c_{\alpha ji} + \frac{2f^n_{\alpha ji} + 5f^c_{\alpha ji} - f^p_{\alpha ji}}{6m_\alpha}\Delta t. \tag{3}$$

Here $x_{\alpha ji}$ is the coordinate i of particle number j of type α, $v_{\alpha ji}$ is the component of the velocity of this particle, $f_{\alpha ji}$ is the ith component of the force which acts on this particle, Δt is the time step of the algorithm; the letter n means ''new,'' c means ''current,'' and p means ''previous.'' This algorithm of second order was used to solve the equations of particles' motion. It is a modification of well known Verlet algorithm and it gives better approximation for velocities [25]. The

forces were calculated via known coordinates using Eq. (1): $f_{\alpha ji}=-\partial U/\partial x_{\alpha ji}$ and taking into account the periodic boundary conditions. It is clear from formulas (3) that one would know the current and previous positions of particles to boot the algorithm. The previous positions were calculated for new particles just as $x^c-v^c\Delta t$.

The fluxes of different species are $J_\alpha=(N_\alpha^{LR}-N_\alpha^{RL})/tA$, where N_α^{LR} (N_α^{RL}) is the number of particles of type α, crossing a given cross section perpendicular to z axis from left-to-right (right-to-left), t is the time passed, and A is the area of cross section.

One can consider the process to be steady when fluxes J_α at different cross sections of the membrane are equal. So, in general,the process was considered to become steady when J_α values at the opposite ends of the membrane (z direction) were within 10% of each other. After that the statistic features were gathered to calculate the permeabilities $K_\alpha=L_1' J_\alpha/\Delta P_\alpha$ of various gases, using stored data, and the dynamic separation factors $S_{\alpha\beta}=K_\alpha/K_\beta$ could be calculated. Here ΔP_α is the differential of partial pressures of species α in the two control volumes. The partial pressures were calculated as $P_\alpha=\langle 2m_\alpha\Sigma_j v_{\alpha j}^z/\Delta tA\rangle$, where $v_{\alpha j}^z$ was the z component of the velocity of the particle j of type α, crossing the outer boundary of the control volume (it was removed from consideration after that); $\langle\cdots\rangle$ denotes the time average. When a steady flow of alkane flow could not be reached during simulation due to CPU time limitations, the upper boundary of $|J_\alpha|$ was calculated as the maximal value of $|J_\alpha|$ at different cross sections of the membrane.

The program, which implements the algorithm described above, uses the cell list technique to reduce calculations (the volume of simulation was divided into cells of r_c size and only the molecules and atoms in this and neighboring cells were taken into account during energy and force calculations). The size of control volumes was chosen so that it was significantly larger than $\max(r_c,d)$ and the number of molecules of each species of gas was at least about 10^2 there.

The program was tested in the limit of ideal gases; the correctness of carbon membrane structure was tested separately. The chemical potentials were chosen so that the concentrations of gases were kept the same during different simulations and were significantly different in the two control volumes.

The thickness of the membrane deserves special discussion. The thickness employed here was $N_1'=6$ (12 graphite planes) and the results were not affected (at the considered level of precision) by decreasing it to eight planes. So this value seems to be a good compromise between the precision of calculations and CPU time consumption. On the other hand, 12 graphite planes represent a distance which is of the order of mesopore sizes (about 4 nm). The distance which separates the closest mesopores might be expected to be of the same order; the mesopores in the real experiment represent the control volumes in numerical simulation. Reproducing the simulation on a different ''sample'' of membrane (having the same pore size distribution) did not significantly affect the permeabilities.

TABLE II. Binary mixtures.

	CH_4	C_2H_6	C_3H_8	i-C_4H_{10}
P_{1H_2}	1.3	1.3	1.3	1.3
P_{2H_2}	0.63	0.62	0.62	0.62
P_{1org}	1.0	0.95	1.1	1.1
P_{2org}	0.48	0.45	0.52	0.54
K_{H_2}	7×10^{-3}	7×10^{-3}	7×10^{-3}	7×10^{-3}
K_{org}	9×10^{-4}	3×10^{-4}	$<5\times10^{-5}$	$<6\times10^{-6}$
S	7	2×10^{1}	$>2\times10^{2}$	$>1\times10^{3}$

III. RESULTS AND DISCUSSION

The primary purpose of this work is to study the transport selectivities of organic molecules and hydrogen under conditions of a real experiment and to consider whether data from single component can predict the behavior of multicomponent systems. Recall that two types of experiments were conducted: single-component transport under a pressure drop and multicomponent diffusion with nitrogen on one side of the membrane and a mixture of hydrogen and alkane on the other side of the membrane. The employed conditions in simulation are dimensionless temperature of $T=25$ (which corresponds to 700 K), membrane porosity $p=0.7$, and average pore size of $d=2.25$ (which corresponds to 0.765 nm). This value is larger, of course, than the size of individual molecules (σ in Table I), but may be smaller than the sum of sizes of two individual gas molecules. The temperature represents the experimental condition. The pore size distribution of the experimental module was measured to be very narrow with 70% of the pore sizes at about 0.6 nm and the rest at 0.8 and 1 nm; the contribution of larger pores was negligible [5]. Both sides were maintained at pressure about a few tens of atmospheres (dimensionless pressure $P=1$ corresponds to 100 atmos).

As expected, large separation between transport of hydrogen and alkane can be achieved and the separation increases with increasing size (or mass) of the alkane molecule (Table I). This is evident from the two-component simulation in which a high chemical potential of the hydrogen and alkane was maintained in one control volume and a low one in the other control volume. The concentrations of H_2 and organic molecules were maintained approximately equal in each control volume in the simulations. Table II lists the diffusing alkane, P_{1H_2} and P_{2H_2} (P_{1org} and P_{2org}) are the corresponding pressures of H_2 (organic gas) in the two control volumes, K_{H_2} and K_{org} are permeabilities of hydrogen and organic gas, and S is the separation factor of hydrogen over the organic gas; all data are in dimensionless units. The figures for permeabilities in the table did not vary upon doubling or halving the ratio of feed concentrations.

The second conclusion is that separations obtained in two- and three-component systems are similar to those obtained from the single-component study. Table III lists analogous simulations of single gases and Table IV presents the separation factor S of hydrogen over alkanes using these single-gases' values. Results show that with the resolution allowed

TABLE III. Single-gas permeabilities.

	H_2	CH_4	C_2H_6	C_3H_8	i-C_4H_{10}
P_1	1.4	1.1	1.1	1.1	1.2
P_2	0.67	0.49	0.50	0.55	0.55
K	7×10^{-3}	9×10^{-4}	1×10^{-4}	$<5\times10^{-5}$	2×10^{-5}

by numerical simulations (explaining the low accuracy listing of the data) the flux (permeability) and selectivities of the binary mixture are not significantly different from those predicted by the single components.

Since nitrogen was the carrier gas in experiments [5], the simulation of ternary gas mixture was implemented in one case: in similarity to experiments the pressure gradient of N_2 was opposite to that of the two other gases — the hydrogen and ethane. The results do not show significant difference from the case of binary mixture (see Table VII).

These transport selectivity results semiquantatively agree with the experiment. Table V lists experimental selectivity values for hydrogen—alkane mixtures at temperature of 673 K (see Ref. [5] for details) as obtained in the three-component study. However, the permeabilities measured experimentally in pure-component studies differ from those in mixtures: Specifically, counterdiffusion of nitrogen and C_2H_6–C_4H_{10} alkanes significantly inhibits the fluxes of both, while hydrogen flux is only slightly diminished [5].

IV. ANALYSIS

The results show that for the predetermined average pore radius employed, the flux of each species is strongly dependent on its molecular size and that the ratio of fluxes (the selectivity) of two components in a mixture is (within experimental simulation accuracy) not significantly different from that obtained from the single components. This result may be accounted for by the pore network with a sieving effect of the pores. The selectivities are different from those expected from Knudsen diffusion (which are $\sqrt{m_{\mathrm{org}}/m_{\mathrm{H_2}}}$, Table VI). These results are different from simulation of diffusion in a single pore [5,12] having a radius of the average pore size employed here, since we cannot sustain the diffusion of two molecules in a single pore, if its cross section is smaller than the sum of the molecule cross sections. The topic of single-file diffusion, especially in zeolites and carbon nanotubes, is currently a topic of extensive investigation (see Ref. [12], and references therein). Transport in single-file diffusion is determined by the molecule size, by its affinity to the surface, and by the energy barrier for diffusion. The latter is small for diffusion in carbon nanotube, which can be argued to be representative of carbon membranes pores [5]. Thus, the selectivity in a hydrogen-hydrocarbon cocurrent diffusion

TABLE IV. Single-gases' based selectivity.

	CH_4	C_2H_6	C_3H_8	i-C_4H_{10}
S	7	5×10^1	$>2\times10^2$	4×10^2

TABLE V. Experimental [5] selectivity.

	CH_4	C_2H_6	C_3H_8	i-C_4H_{10}
S	4.1	5×10^1	$>4\times10^2$	$>4\times10^2$

in a single pore will be determined by the pore size. In a pore network we can find phase separation in a way that the smaller pores convey hydrogen while the larger ones transport hydrocarbon. Consequently, hydrocarbon flux may not be significantly diminished, in comparison with fluxes in a single-component system. Hydrogen molecules may hop over the hydrocarbon molecules, even at smaller pores and their flux will not be diminished significantly. Thus, the selectivity will not be affected considerably.

Thus, the pore size distribution is important in determining the selectivity, and we derive below a simple model to that effect which integrates the Poisson distribution of pore sizes along with the asymptotic Knudsen selectivities at large pores. Assume that the porosity is well above the percolation threshold of either species (only in this case one can hope that transport occurs). The concentration of gases is small, so we can treat each gas independently. In this case the flux is inversely proportional to the square root of the mass of gas molecules (Knudsen diffusion) and to the total cross section of pores open for the diffusion. The latter is assumed to be proportional to the number of the pores available for the gas (i.e., that are larger than the molecules). If the temperature is high, then the effect is purely geometrical. Taking into account the assumed Poisson distribution of the number n of removed adjacent carbon atoms inside pores $p_n = \bar{n}^n/n!e^{-\bar{n}}$, where $\bar{n}=\pi/6\rho_c d^3$ is average n, we have

$$S_{12}=\sqrt{\frac{m_2}{m_1}}\frac{p(1)}{p(2)}, \tag{4}$$

where $p(k)=p\Sigma_{n=n_k}^{\infty}p_n$, $p(k)$ is porosity, available for given molecule size, $n_{1,2}=\pi/6\rho_c[2^{1/6}(\sigma_c+\sigma_{1,2})]^3$ are the cutoff values, and $\rho_c=1.49$ is the concentration of carbon atoms (in dimensionless units). In other words, the value of $p(k)$ is the total porosity times the probability that the pores are large enough. Multiplier $\pi/6$ appears here due to spherical shape of the pores, $2^{1/6}(\sigma_c+\sigma_{1,2})$ is the doubled equilibrium distance between the carbon atom and a gas molecule. This number is the diameter of the smallest pore, where a gas molecule may reside loosely.

The cutoff values of the various molecules are marked in Fig. 2 showing that the available porosity, which is depen-

TABLE VI. Knudsen and "theoretical" selectivity.

	CH_4	C_2H_6	C_3H_8	i-C_4H_{10}
$\sqrt{\frac{m_{\mathrm{org}}}{m_{\mathrm{H_2}}}}$	3	4	4	5
S	7	3×10^1	4×10^2	1×10^3

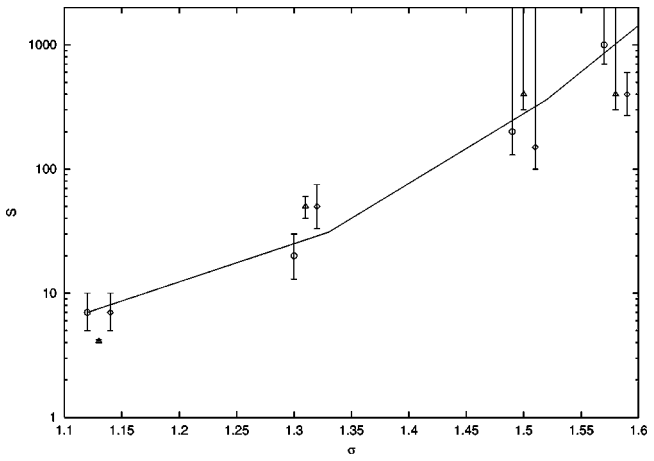

FIG. 3. Dependence of hydrogen-alkane separation factor *S* on the alkane molecular size (σ) ("○" denotes simulated values of binary mixtures, "◇" denotes simulated values of single gases, "△" denotes the experimental values [5] at 673 K, solid line denotes theoretical curve, and bars denote errors estimated from reproducible experiments).

dent on molecule size, is relatively large for hydrogen and extremely small for propane and butane. Recall that percolation threshold is specified by the porosity, and although the porosity available for the large molecules is probably below the threshold, the small sample size (thickness) and the periodic boundary conditions allow for fluxes of propane and butane. This crude model predicts (Table VI) a low value for separation factor which tends to Knudsen in the case of an average pore size that is larger than both molecular sizes and a very high value for separation factor when the molecular size of one component of the mixture is larger than average pore size. If we roughly assume that the mass of an alkane molecule is proportional to its σ^3, then Eq. (4) predicts dependence of *S* (alkane with respect to hydrogen) on σ, which is presented at Fig. 3 together with the data from simulation and experiment. We should stress that Eq. (4) explains the behavior of the separation factor only to a first approximation. Its ability to predict well the simulated results suggests that accounting for long narrow pores, which are dominated by energetic effects, will not affect the result significantly. This result may differ in less-porous and larger systems.

The corrections due to finite temperature are determined by the ratio E_{12}/T, where E_{12} is the difference of the activation energies of gas species 1 and 2 in the pores. This value strongly depends on specific membrane structure. For example, it will be 20 times larger or so than $\sqrt{\epsilon_c}(\sqrt{\epsilon_1}-\sqrt{\epsilon_2})/T$ in the case of the cylindrical narrow pore due to simultaneous interaction with carbon atoms of the pore wall around. However, in the considered case of porous network, such simultaneous interactions with many carbon atoms should happen less frequently because there is no smooth wall near the gas molecules. So, the ratio E_{12}/T should be about $\sqrt{\epsilon_c}(\sqrt{\epsilon_1}-\sqrt{\epsilon_2})/T$ which is small for the studied gases and temperatures about room and higher. The numerical simulation confirms that the correction is small (see Table VII). In general, the calculation of the correction is not simple [11,26]. These arguments explain why the behavior in narrow carbon nanotube is completely different: molecular mechanics simulations of small alkane molecules through such structures exhibit very strong interactions, suggesting that in most cases desorption is the rate determining step [5]. This calls for a microscopic study of the membrane structure in order to determine the most appropriate model for simulations.

V. CONCLUSION

The numerical simulation of nonequilibrium cotransport of H_2 and alkane gas mixtures with very different molecular sizes through a porous carbon membrane structure was implemented. For the highly porous network, the simulated selectivities in binary diffusive systems (and in one ternary system) can be predicted from single-gas permeabilities. This suggests that the effect is geometrical, and an approximate model of the transport is proposed. It can be used for an estimation of the separation factor of a membrane. Simulations are compared with experimental results of two- and three-component codiffusion and counterdiffusion in a carbon membrane. The simulations predict well the ratio of single component permeabilities, but they do not predict the mutual inhibition of fluxes in counter-diffusion. These results differ also from predictions of diffusion in narrow carbon-nanotubes, where energetics effects were found to determine

TABLE VII. Comparison of permeabilities in single-, binary-, and ternary-gas simulations.

Conditions	P_{1H_2}	P_{2H_2}	$P_{1C_2H_6}$	$P_{2C_2H_6}$	P_{1N_2}	P_{2N_2}	K_{H_2}	$K_{C_2H_6}$	K_{N_2}
$T=25;H_2$	1.4	0.67					6×10^{-3}		
$T=25;H_2$	1.4	0.72				9×10^{-3}			
$T=25;C_2H_6$			1.1	0.50				2×10^{-4}	
$T=25;N_2$					0.42	0.93			6×10^{-4}
$T=25;H_2$ and C_2H_6	1.3	0.62	0.95	0.45			7×10^{-3}	5×10^{-4}	
$T=10;H_2$ and C_2H_6	1.3	0.69	0.61	0.34			8×10^{-3}	3×10^{-4}	
$T=25;H_2$ and C_2H_6	0.60	0.28	0.99	0.44			7×10^{-3}	2×10^{-4}	
$T=25;H_2,C_2H_6,N_2$	1.3	0.60	0.93	0.42	0.36	0.84	7×10^{-3}	2×10^{-4}	8×10^{-4}

[a]Another sample of membrane.

the selectivities. But, the results of a nanotube network study are expected to be different. The uniqueness of this work lies in the comparison of simulated, approximate, and experimental results, which enables us to identify the important parameters. Extending these results to less-porous systems will reveal the impact of energetic effects.

ACKNOWLEDGMENTS

The authors would like to thank Dr. I. Efremenko for useful discussions. This work was supported by the Ministry of Science of Israel and I.K. was partially supported by Israel Council for Higher Education.

[1] T.J. Pinnavaia and M.F. Thorpe, in *Access in Nanoporous Materials* (Plenum, New York, 1995).
[2] C.W. Jones and W.J. Koros, Carbon **32**, 1419 (1994); **32**, 1427 (1994).
[3] H. Hatoi, Y. Yamada, and M. Shiraish, Carbon **30**, 763 (1992).
[4] F.G. Emmerich, Carbon **33**, 1709 (1995).
[5] G.A. Sznejer, I. Efremenko, and M. Sheintuch, AIChE J. (to be published).
[6] G.S. Heffelfinger and F. van Swol, J. Chem. Phys. **100**, 7548 (1994).
[7] T. Nitta, M. Nozawa, and Y. Hishikawa, J. Chem. Eng. Jpn. **28**, 267 (1995).
[8] D.M. Smith, AIChE J. **32**, 329 (1986).
[9] M. Sun and C. Ebner, Phys. Rev. A **46**, 4813 (1995).
[10] A.P. Thompson, D.M. Ford, and G.S. Heffelfinger, J. Chem. Phys. **109**, 6406 (1998).
[11] L. Xu, M. Sahimi, and T.T. Tsotsis, J. Chem. Phys. **112**, 910 (2000).
[12] Z. Mao and S.B. Sinnott, J. Phys. Chem. B **105**, 6916 (2001).
[13] S.K. Bhatia and D. Nicholson, Phys. Rev. Lett. **90**, 016105 (2003).
[14] K.D. Travis and K.E. Gibbins, Mol. Simul. **25**, 209 (2000).
[15] L. Xu, M. Sahimi, and T.T. Tsotsis, Phys. Rev. E **62**, 6942 (2000).
[16] J. Wood, L.F. Gladden, and F.J. Keil, Chem. Eng. Sci. **57**, 3047 (2002).
[17] X. Yi, K.S. Shing, and M. Sahimi, AIChE J. **41**, 456 (1995); Chem. Eng. Sci. **51**, 3409 (1996); X. Yi, J. Ghassemzadeh, K.S. Shing, and M. Sahimi, J. Chem. Phys. **108**, 2178 (1998); J. Ghassemzadeh, L. Xu, T.T. Tsotsis, and M. Sahimi, *ibid.* **108**, 2178 (1998); J. Phys. Chem. B **104**, 3892 (2000).
[18] L. Xu, M. Sahimi, and T.T. Tsotsis, J. Chem. Phys. **114**, 7196 (2001).
[19] Z. Mao and S.B. Sinnott, Phys. Rev. Lett. **89**, 278301 (2002).
[20] M. Lupkowski and F. van Swol, J. Chem. Phys. **95**, 1995 (1995).
[21] J.M.D. MacElroy, J. Chem. Phys. **101**, 5274 (1994).
[22] T. Düren, F.J. Keil, and N.A. Seaton, Fundam. Adsorption **7**, 442 (2002).
[23] M.G. Sedich, M. Jahangiri, P.K.T. Liu, M. Sahimi, and T.T. Tsotsis, AIChE J. **46**, 2245 (2000).
[24] *Handbook of Physics*, edited by E.U. Condon and Hugh Odishaw (McGraw-Hill, New York, 1958).
[25] D. Frenkel and B. Smit, *Understanding Molecular Simulation: From Algorithms to Applications* (Academic Press, San Diego, 1996).
[26] M. Acharya and H.C. Foley, AIChE J. **46**, 911 (2000).